Various 3*d*-4*f* spin interactions and field-induced metamagnetism in the Cr^{5+} system $DyCrO_4$

Youwen Long,* Qingqing Liu, Yuxi Lv, Richeng Yu, and Changqing Jin†

National Laboratory for Condensed Matter Physics, Institute of Physics, Chinese Academy of Sciences, Beijing 100190, China

(Received 4 November 2010; revised manuscript received 30 November 2010; published 31 January 2011)

A tetragonal zircon-type $DyCrO_4$ with space group $I4_1/amd$ was prepared at ambient pressure. By quenching this zircon phase from 6.0 GPa and 720 K, another tetragonal scheelite-type $DyCrO_4$ was obtained with the reduction of lattice symmetry to $I4_1/a$. Both phases contain spatially separated CrO_4 tetrahedra with rare Cr^{5+} state and Cr-O-Dy-O-Cr spin interaction chains. In the zircon phase, significantly different Cr-O-Dy bond angles were found along different lattice axes, giving rise to ferromagnetic and antiferromagnetic interactions around 23 and 21 K, respectively. Due to magnetic frustration caused by the competitive ferromagnetic and antiferromagnetic interactions, a field-induced metamagnetic transition took place at a small field about 0.15 T. In the scheelite phase, antiferromagnetic ordering occurred below 24 K. Similar to the zircon phase, field-induced metamagnetism was also observed in the scheelite-type $DyCrO_4$, but at a higher field of about 3.0 T. Possible orbital ordering was discussed in the high-pressure scheelite phase.

DOI: 10.1103/PhysRevB.83.024416 PACS number(s): 75.30.Kz, 75.30.Et, 81.40.Vw

I. INTRODUCTION

Mixed-metal oxides *R*-TM-O (*R* = alkaline or rare-earth metals, TM = transition metals) systems exhibit a wide variety of structural, magnetic, and transport properties due to strong correlation and coupling between lattice, charge, spin, and orbital degrees of freedom. In these systems, perovskite and perovskite-related oxides have received special attention due to their interesting physical properties such as high-T_c superconductivity, colossal magnetoresistance, magnetic ferroelectricity, and intermetallic charge transfer.[1–4] For ABO_3-type perovskite oxides, material magnetism is often dominated by *B*-site TM ions, even though magnetic rare-earth ions are involved in the *A* site. In 3*d* electronic systems, the Anderson-Goodenough-Kanemori (AGK) empirical rules point out that the *B*-O-*B* superexchange interaction would lead to an antiferromagnetic (AFM) state when ∠*B*-O-*B* is close to 180°, whereas it would lead to a ferromagnetic (FM) state when the angle is close to 90°.[5–7] Compared to the *d* electrons, the orbital configurations of *f* electrons are more complex and little is known about the magnetic interactions between *f*-*f* and *d*-*f* electrons. It is therefore desirable to find an appropriate material system and study the spin interactions of *f*-*d* electrons.

ABO_4-type $Ln^{3+}Cr^{5+}O_4$ (Ln = lanthanide and Y) belongs to the family of mixed-metal oxides, where magnetic ions appear in both *A* and *B* sites. These compounds (except for Ln = La and Ce) crystallize to a tetragonal zircon-type structure with space group $I4_1/amd$ (No. 141, $Z = 4$) at ambient conditions. The crystal structure consists of CrO_4 tetrahedra and LnO_8 bisdisphenoid polyhedra. As shown in Fig. 1(a), LnO_8 units connect with one another along the *x* and *y* axis by sharing O-O edges, whereas they alternately align with CrO_4 units along the *z* axis. In zircon-type $LnCrO_4$, therefore, the *B*-site CrO_4 units are spatially isolated by LnO_8 units. As a result, Cr-O-Ln-O-Cr super-superexchange interaction occurs, which should be responsible for the magnetic properties. Thus, $LnCrO_4$ is an ideal family to study 3*d*-4*f* spin interactions.

However, the crystal structure of zircon-type $LnCrO_4$ is rather sensitive to external conditions. Structural phase transitions have been found in several $LnCrO_4$ compounds at low temperatures.[8–11] Under high pressure, the tetragonal zircon phase seems to change constantly to another tetragonal scheelite phase with symmetry reduction from $I4_1/amd$ to $I4_1/a$ (No. 88, $Z = 4$).[12] This pressure-induced structural phase transition is irreversible with considerable volume contraction as large as ∼10%, suggesting its first-order nature.[13] In spite of the large unit cell volume collapsing during transition, the coordination polyhedra (CrO_4 and LnO_8) are almost unchanged and the CrO_4 tetrahedra are still separated from one another.[14,15] As shown in Fig. 1(b), CrO_4 and LnO_8 units alternately align along the *x* and *y* axes in the scheelite phase. Along the *z*-axis direction, two edge-sharing LnO_8 form a dimmer that alternately connects with CrO_4. However, the structural rearrangement caused by the first-order structural transition gives rise to considerable change in Ln-O-Cr angle.[15] Since both 3*d*- and 4*f*-electrons take part in the magnetism, it is possible to see the sign change of spin interaction when structural transition occurs. Therefore, $LnCrO_4$ opens up an opportunity to study magnetic dependence on different 3*d*-4*f* interaction pathways.

In this paper, we report the synthesis and complex magnetism closely related to 3*d*-4*f* electronic interactions in both ambient-pressure zircon-type and high-pressure scheelite-type $DyCrO_4$. Different orbital overlapping between the 3*d*-Cr^{5+} and 4*f*-Dy^{3+} ions result in different spin interactions in these two isomorphic compounds, and both of them exhibit field-induced metamagnetic transitions.

II. EXPERIMENT

We prepared the zircon-type polycrystalline sample at ambient pressure and a relatively low temperature (<800 K) using highly pure $Dy(NO_3)_3{\cdot}6H_2O$ and $Cr(NO_3)_3{\cdot}9H_2O$ as starting materials. Appropriate reagents were completely mixed, and then a heat treatment as used for the synthesis of zircon-type $YCrO_4$ was carried out.[14] To obtain the high-pressure scheelite phase, the zircon phase with green color was treated at 6.0 GPa and 720 K for 15 min using a cubic anvil-type high-pressure apparatus.[16] The as-made scheelite phase was black and both the zircon and scheelite phases were insulating. X-ray diffraction (XRD) was performed at room temperature (RT) using a Rigaku diffractometer (Cu $K\alpha$ radiation, 40 kV, 300 mA) from 15 to 135° with a

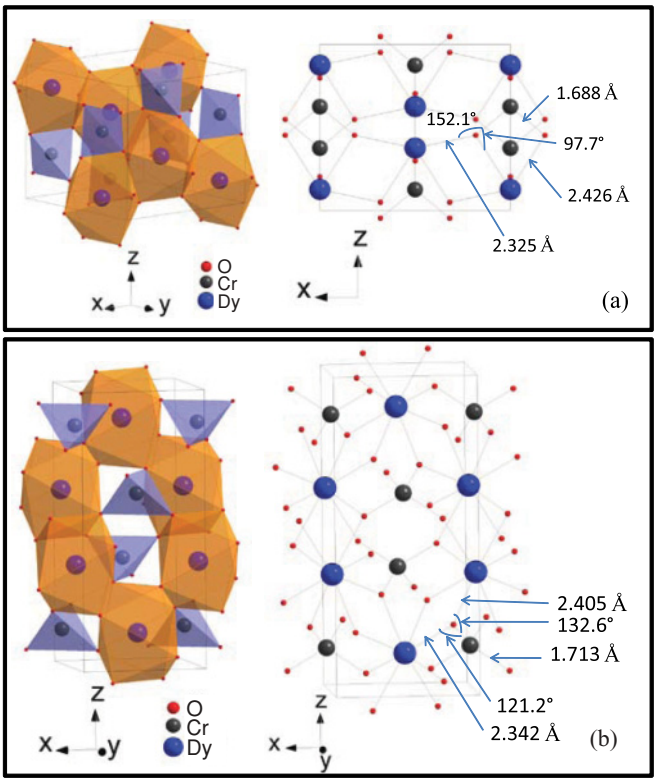

FIG. 1. (Color online) Crystal structure and atomic connection network of (a) zircon-type and (b) scheelite-type $DyCrO_4$.

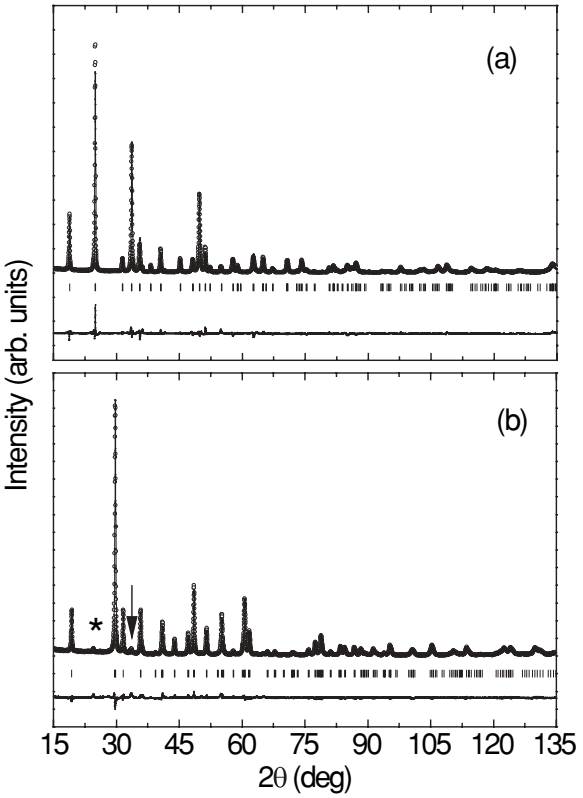

FIG. 2. XRD patterns and the Rietveld refinement profiles of (a) zircon-type and (b) scheelite-type $DyCrO_4$ at RT. The asterisk and arrow in (b) show the residual zircon-type $DyCrO_4$ and $DyCrO_3$ impurities, respectively.

step of 0.02°. The GSAS program was applied to refine the structural parameters by the Rietveld method.[17] To examine the oxygen content, thermogravimetry (TG) measurement was made from RT to 1273 K at a heating rate of 10 K/min and in an ambient atmosphere using a Rigaku TG-DTA 8120 system. The dc magnetic susceptibility (χ_{dc}) and low-field ($\leqslant$ 3 T) magnetization (M) were measured using a commercial superconducting quantum interference device magnetometer. Zero-field-cooled (ZFC) and field-cooled (FC) modes were used to measure χ_{dc} at different magnetic fields (Hs). A ZFC mode was used to measure M-H curves. The data of ac susceptibility (χ_{ac}), specific heat (C_p), and high-field magnetization up to 12 T were collected on a physical property measurement system.

III. RESULTS AND DISCUSSION

As shown in Fig. 2(a), the XRD pattern of the $DyCrO_4$ synthesized at ambient pressure can be well fit based on a zircon-type $I4_1/amd$ structural symmetry with lattice parameters $a = 7.1364(2)$ and $c = 6.2687(2)$ Å. In this symmetry, Dy and Cr atoms are respectively located at special sites 4a (0,3/4,1/8) and 4b (0,1/4,3/8), and O occupies 16h site [0,0.4314(6),0.2020(6)]. After quenching the zircon phase from high pressure, the Rietveld analysis shows that the structure changes to a scheelite-type new phase with $I4_1/a$ symmetry [Fig. 2(b)], and the lattice constants are $a = 5.0157(1)$ and $c = 11.3196(3)$ Å. Correspondingly, the atomic positions are restructured at 4b (0,1/4,5/8) for Dy, 4a (0,1/4,1/8) for Cr, and 16f [0.2611(9),0.1124(8),0.0488(4)] for O. Some refinement structural data for these two phases are given in Table I. During the structural phase transition, although the material's density significantly decreases by about 13.6%, only tiny variations occur in both Cr-O and Dy-O distances. However, the connection between CrO_4 and DyO_8 units characterized by ∠Dy-O-Cr changes strikingly (Table I). This considerable variation will affect magnetic interaction between the 3d-Cr^{5+} and 4f-Dy^{3+} ions. Note that small amounts of impurity phases (<5%) including the residual zircon-type $DyCrO_4$ and $DyCrO_3$ are identified in the high-pressure scheelite phase, but these do not affect the material's intrinsic magnetism.

In the present $DyCrO_4$, the valence state of Cr^{5+} is very rare. This unusual ionic state is sensitive to high temperature and the compound will decompose to a refractory $DyCrO_3$ perovskite phase when the temperature is high enough. Figure 3 shows the TG measurement result of the zircon-type $DyCrO_4$. The slight TG decrease

TABLE I. Refinement structural data of zircon- and scheelite-type $DyCrO_4$.

Phase	Cr-O (Å)	O-Cr-O (°)	Dy-O (Å)	Dy-O-Cr (°)	R_{wp} (%)	R_p (%)
Zircon	1.688(4)	100.2(3)	2.325(4)	97.7(2)	11.45	8.64
		114.3(1)	2.426(4)	152.1(2)		
Scheelite	1.713(4)	119.6(3)	2.342(4)	132.6(2)	7.96	6.14
		104.7(1)	2.403(4)	121.2(2)		

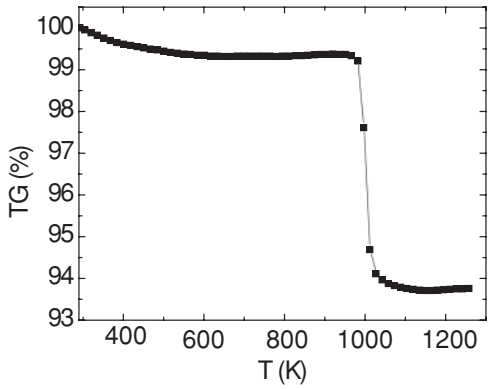

FIG. 3. Temperature dependence of TG curve of zircon-type $DyCrO_4$.

below ~600 K is ascribed to the absorption vapor on the sample surface. The compound looks stable below 980 K, but above that temperature, it decomposes to $DyCrO_3$ with a weight loss of about 5.67%. This value is consistent with theoretical oxygen loss (5.75%) in the decomposed reaction $DyCrO_4 \rightarrow DyCrO_3 + 1/2O_2$, confirming the stoichiometry of our $DyCrO_4$ sample within experimental error (<1%). Besides, during the structural refinement, we did not find any anomaly for the occupation factors, even for the O atom. It also suggests that the chemical composition of the present $DyCrO_4$ is stoichiometric, in agreement with the TG measurement result.

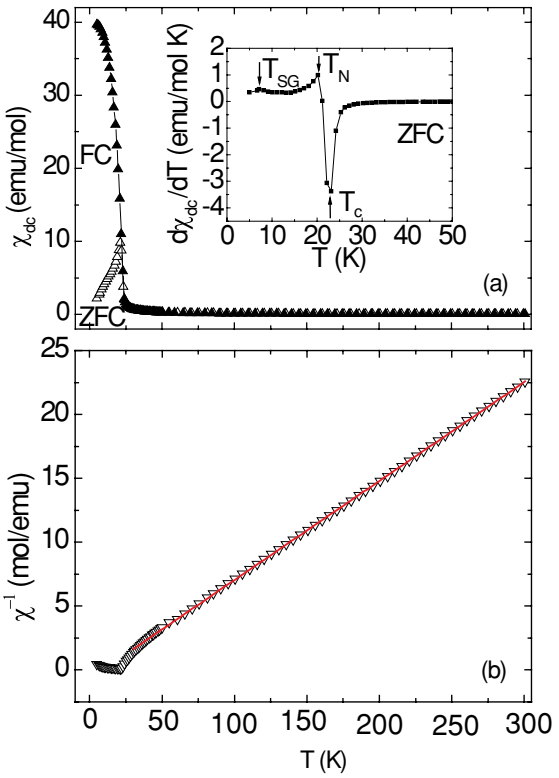

FIG. 4. (Color online) Temperature dependence of (a) ZFC and FC dc susceptibility and (b) inverse ZFC dc susceptibility of zircon-type $DyCrO_4$ at 5 mT. The inset in (a) shows the derivative of ZFC susceptibility.

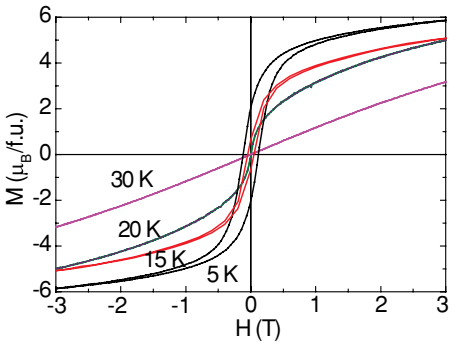

FIG. 5. (Color online) Magnetization curves of zircon-type $DyCrO_4$ at different temperatures.

Figure 4(a) shows the magnetic susceptibility of the zircon-type $DyCrO_4$. It sharply increases as temperature decreases to ~23 K due to a paramagnetic (PM)-to-FM transition as confirmed by neutron diffraction.[10,11] Following that, a steep drop occurs in the ZFC susceptibility curve around 21 K. We assign this anomaly as an AFM transition. In this study, the FM Curie temperature (T_C) and the AFM Néel temperature (T_N) were determined from the T-$d\chi_{ZFC}/dT$ curve as shown in the inset of

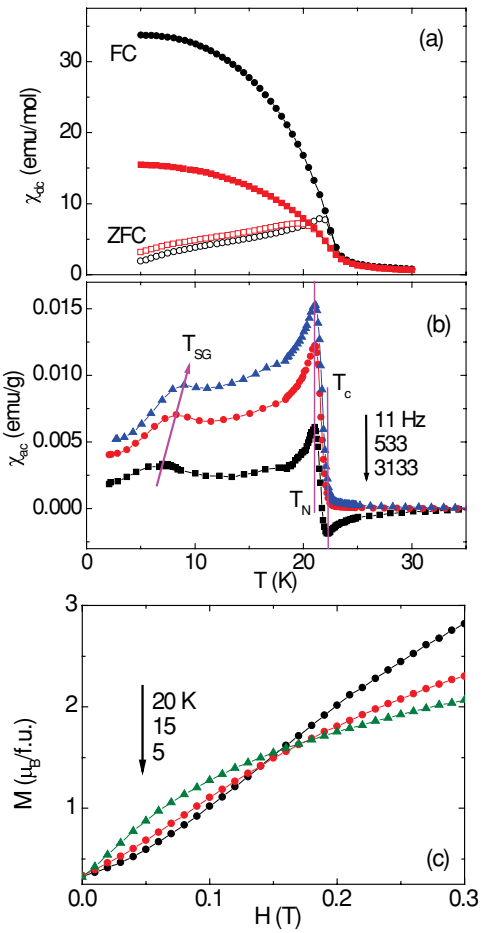

FIG. 6. (Color online) Temperature dependence of (a) dc susceptibility measured at 10 mT (circles) and 50 mT (squares) and (b) the imaginary part of ac susceptibility at different frequencies; (c) magnetization curves measured at low fields in the zircon-type $DyCrO_4$.

Fig. 4(a), where a third anomaly was found around $T_{SG} = 7$ K. This anomaly is attributed to a spin glass (SG) transition originating from the competitive FM and AFM interactions as will be discussed later. Above 30 K, the susceptibility data can be well fit using the Curie-Weiss law [see Fig. 4(b)], producing a positive Weiss constant (8.3 ± 0.2 K), as expected from the FM transition, and an effective moment of $10.18\mu_B$. This moment is very close to the theoretical value of $10.77\mu_B$, when we consider the orbital moment contribution of a $4f$-Dy^{3+} ion and spin only contribution of a $3d$-Cr^{5+} ion with spin $S = 1/2$.[8]

Corresponding to the PM state, linear magnetization behavior is observed at 30 K (Fig. 5). Below the T_C, however, magnetic hysteresis loops emerge with a saturated moment of $\sim 6.0\mu_B$/f.u. at 5 K and 3.0 T. This value is clearly larger than the saturated moment of a free $3d$-Cr^{5+} ion ($1.0\mu_B$), so the $4f$-Dy^{3+} ions should be involved in the FM interaction. Actually, neutron diffraction revealed that the Cr^{5+} and Dy^{3+} spin sublattices were ferromagnetically coupled at the T_C.[10,11]

It should be noted that the magnetic property presented in the zircon-type $DyCrO_4$ is essentially different from a conventional canted AFM ordering in that this material shows significant glassy magnetic behavior and metamagnetism. This is related to the competitive FM and AFM interactions. For example, as shown in Fig. 6(a), T_N is strongly dependent on the applied field. With increasing field, it gradually shifts toward a low temperature and the ZFC and FC curves tend to be uniform. The SG behavior is further confirmed by a frequency-dependent cusp around T_{SG} in ac susceptibility [Fig. 6(b)]. In sharp contrast, T_C and T_N are almost frequency independent. In neutron diffraction, the AFM ordering, which appeared below the T_C, could not be distinguished from the FM ordered state.[10,11] This is probably due to the weakness of AFM reflection and/or its overlapping with the FM reflection. In accordance with the metamagnetism, S-type magnetization curves are observed at low temperatures, such as 5 and 15 K, with curvature changes around 0.15 T [Fig. 6(c)]. This field was defined as the critical field for the metamagnetic transition.

The susceptibility data of the scheelite-type $DyCrO_4$ in Fig. 7(a) indicates that an AFM transition takes place at $T_N' \sim 24$ K, which is also the onset of deviation between the ZFC and FC susceptibility curves as presented in the inset. With decreasing temperature, another kink occurs around 18 K, but no λ-type anomaly is observed in specific heat (Fig. 9). This anomaly is probably indicative of a temperature dependence of molecular field, as reported in the isostructural compound $TbCrO_4$.[18] The small increase of susceptibility below 8 K is thought to be related to the small amounts of impurity phases. The temperature dependence of susceptibility above 30 K could be well reproduced by the Curie-Weiss law [Fig. 7(b)]. A negative Weiss constant (-1.5 ± 0.4 K) was obtained, implying AFM interaction at low temperature. The fitted effective moment ($10.27\mu_B$) is almost the same as that obtained in the zircon phase ($10.18\mu_B$), and consistent with the theoretical value ($10.77\mu_B$).

In agreement with the AFM ordering, linear M-H curves are observed below the T_N' at low field (<2.0 T), as shown in the inset of Fig. 8. However, the scheelite-type $DyCrO_4$ also exhibits field-induced metamagnetism. As seen from Fig. 7(a) and the inset, below 50 mT, the AFM transition is robust and the ZFC and FC curves separate from each other, below T_N'. With the field up to 1.0 T, these two curves nearly overlap, but the AFM transition still exists. At 4.0 T, however, the susceptibility monotonously increases with decreasing temperature and no AFM sign is discernible. To explore this field-induced metamagnetism, we measured the magnetization with the field up to 12 T. As shown in Fig. 8, the M-H curves clearly deviate from the linear behavior and the M steeply increases around 3.0 T at low temperatures.

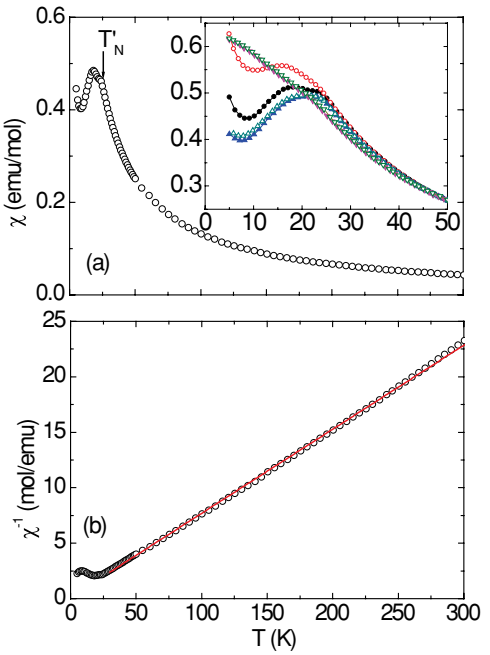

FIG. 7. (Color online) Temperature dependence of (a) magnetic susceptibility and (b) inverse susceptibility of scheelite-type $DyCrO_4$ at 10 mT. The inset of (a) shows the susceptibility obtained at 50 mT (circles), 1.0 T (up triangles), and 4.0 T (down triangles). The solid and open symbols present ZFC and FC curves, respectively.

Specific heat gives additional information on the magnetism of the scheelite-type $DyCrO_4$. Figure 9 shows the C_p data measured at 0 and 10 T. Corresponding to the AFM transition around 24 K, a λ-type anomaly occurs in the zero-field C_p curve. Due to the metamagnetic transition, at 10 T, this anomaly disappears instead of broadening its peak around 15 K. Because the material is an electrical insulator, only the

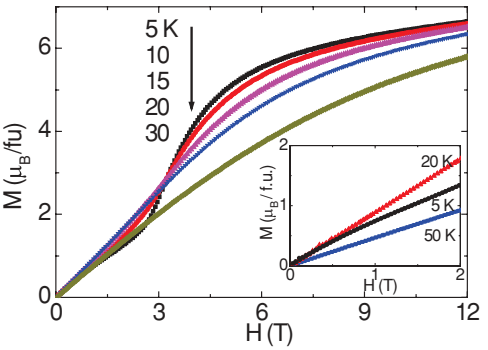

FIG. 8. (Color online) High-field magnetization curves of scheelite-type $DyCrO_4$. The inset shows the linear magnetization behavior at low field.

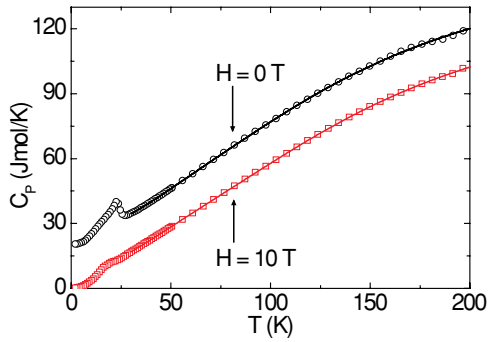

FIG. 9. (Color online) Temperature dependence of specific heat of scheelite-type $DyCrO_4$ at zero field (circles) and 10 T (squares). For clarity, the data at 0 T was shifted by 20 units along the y axis. The solid curves show the fitting results from the Einstein model.

phonon contributes to C_p in the PM state. The C_p data above 30 K, therefore, can be well fit using the Einstein model at zero field and 10 T,[14] as shown by the solid curves in Fig. 9. Since the phonon as well as the AFM excitation contribution to C_p is proportional to T^3, a linear C_p-T^3 behavior below $T_N' \approx$ 24 K is expected at zero field. As shown in Fig. 10(a), this linear behavior is observed between 18 and 24 K. However, it deviates below 18 K due to the molecular field effect, which is characterized by a weak shoulder in the zero-field C_p curve, as discovered in the scheelite-type $TbCrO_4$.[18] At 10 T, this effect looks as if it has been ruled out, and a nice fit is obtained using the function $\alpha T^3 + \beta T^{3/2}$ [Fig. 10(b)]. The fitted parameters are $\alpha = 0.00\,123(7)$ J mol K^{-4} and $\beta = 0.071(4)$ J mol $K^{-5/2}$. The contribution of the $T^{3/2}$ term is attributed to the FM component caused by the field-induced metamagnetism.

The magnetic origin of $DyCrO_4$ is rather complex because several possible super-superexchange pathways are involved. In Fig. 1, we plot the atomic connection network to clarify possible magnetic interactions. For the zircon-type $DyCrO_4$, two kinds of zigzag chains, Dy-O-Dy-O-Dy ($J1$) and Cr-O-Dy-O-Cr ($J2$), are presented along the x axis. Along the z axis, there are two identical Cr-O-Dy-O-Cr ($J3$) chains. In the isostructural compounds $DyVO_4$ and $DyAsO_4$ without magnetic ions in the 4b site, AFM orderings caused by $J1$ are found but the transition temperatures (<3.5 K) are much less than the T_N and T_C observed in $DyCrO_4$.[19,20] The interaction energy of $J1$ is therefore negligible compared to $J2$ and $J3$ in the present $DyCrO_4$. In $J2$ and $J3$, the Cr-O distances are identical and the Dy-O distances are also comparable (Table I). This could be the reason for T_C and T_N's closeness. However, a significant difference between $J2$ and $J3$ is the bond angle of Cr-O-Dy. It is 152.1° in $J2$ and 97.7° in $J3$. These significant different bond angles will lead to essential different orbital overlapping between the 3d-Cr^{5+} ions and the 4f-Dy^{3+} ions, and thereby different magnetic interactions. Since the amount of $J3$ is double that of $J2$, the total interaction energy of $J3$ should be stronger. We therefore temporarily conclude that $J3$ with $\angle$Cr-O-Dy $\approx$ 97.7° contributes to the FM transition around 23 K, and $J2$ with $\angle$Cr-O-Dy $\approx$ 152.1° contributes to the AFM transition around 21 K. This assignment is in agreement with the AGK empirical rules, which are widely used to describe the magnetism of d-electron

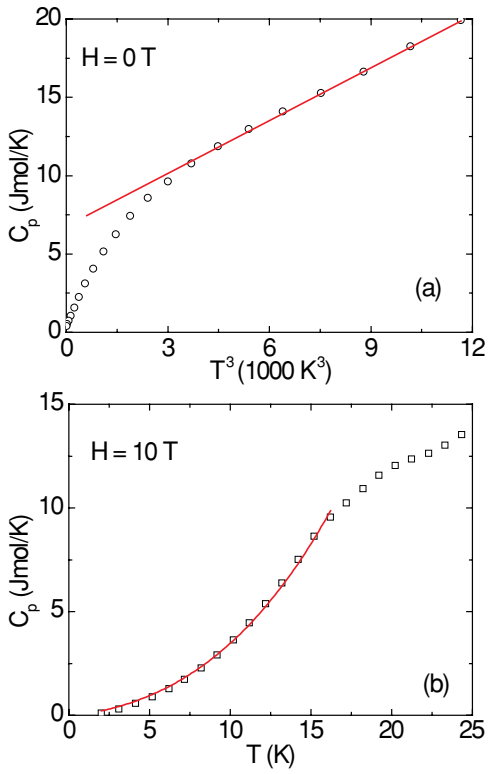

FIG. 10. (Color online) Low-temperature specific heat data of scheelite-type $DyCrO_4$. (a) C_p-T^3 relationship at 0 T, and the solid line shows a linear fitting between 18 and 24 K. (b) C_p-T relationship at 10 T, and the solid curve gives a nice fitting using the function $\alpha T^3 + \beta T^{3/2}$.

systems, although f electrons are involved in the present $DyCrO_4$.

With decreasing temperature to T_C, $J3$ starts to play a role on magnetism, and Cr^{5+} and Dy^{3+} spin sublattices are coupled to each other by FM interaction. Once the temperature decreases to T_N, $J2$ also takes part in the magnetic interaction and spin-frustrated behavior emerges due to different magnetic coupling results from $J2$ and $J3$. Therefore, the magnetism below T_N is strongly dependent on the external field so that a small field (~0.15 T) is enough to induce a metamagnetic transition. In fact, field-induced metamagnetism was also reported on other zircon-type $LnCrO_4$ at low fields with Ln = Gd, Tb, Tm, and Yb, but there was no explanation on the origin.[21] We believe that the same mechanism proposed in this study should exist in those isostructural compounds. In addition, to explain the complex magnetism of the $LnCrO_4$ family, a Cr-O-O-Cr interaction pathway was suggested.[22] However, the O-O distance in this pathway is rather large (about 3.0 Å), and the interaction intensity should be quite small compared to that of Cr-O-Ln-O-Cr. Hence, we did not consider the Cr-O-O-Cr interaction in the present $DyCrO_4$. Note that a second-order structural transition from tetragonal to orthorhombic phase occurs in the zircon-type $DyCrO_4$ around 32 K,[8,10] but only tiny changes occur in bond lengths and angles. We therefore use the zircon phase to describe the magnetism and compare it with the scheelite phase in a tetragonal framework.

The atomic connection network for the high-pressure scheelite-type $DyCrO_4$ is presented in Fig. 1(b). There is

only one Cr-O-Dy-O-Cr chain along the *x*- axis or the *z* axis. Compared to the zircon phase, the difference of bond angle (∠Cr-O-Dy) along different lattice directions is considerably reduced. Specifically, the angle is 121.2° along the *x* axis (*J*2') and 132.6° along the *z*- axis (*J*3'). Recently, an *A*-type-like AFM structure was determined in the scheelite-type $TbCrO_4$.[18] By comparison, a similar magnetic structure is expected in the ground state of the scheelite-type $DyCrO_4$. It means that the spin moments of Dy^{3+} and Cr^{5+} ions, which lie in *ab* planes with $z = 1/8$, $3/8$, $5/8$, and $7/8$, ferromagnetically align in a specific *ab* plane, and the nearest neighboring FM layer is antiferromagnetically coupled along the *z* axis. In this scenario, *J*2' yields a FM interaction in plane, whereas *J*3' yields an AFM interaction out plane in the scheelite-type $DyCrO_4$. At present, we do not exactly know the origin of the field-induced metamagnetism in the high-pressure scheelite phase, but it should be closely related to this specially ordered spin ground state.

In the well-known perovskite oxide $LaMnO_3$, the *A*-type AFM ordering is associated with an orbital ordering of e_g electrons of Mn^{3+} ions.[23] In the present $DyCrO_4$, the e_g orbitals are also occupied by $3d^1$ electrons of Cr^{5+} ions taking into account the presence of a tetrahedral crystal field. Although the Cr-O distances are identical in a CrO_4 tetrahedron, there are two different kinds of O-Cr-O angles which differ by ~12% (Table I). It means that the e_g orbital is probably nondegenerated due to the Jahn-Teller effect. So the *A*-type-like AFM ground state in the scheelite-type $DyCrO_4$ is also possible to couple with an orbital ordering.

IV. CONCLUSION

In conclusion, we prepared the zircon-type and the scheelite-type $DyCrO_4$. In these two phases, CrO_4 tetrahedra were spatially isolated by DyO_8 units, and Cr-O-Dy-O-Cr spin interaction chains dominated the magnetism. In the zircon phase, the Cr-O-Dy bond angles along different lattice axes were considerably different, and FM transition with ∠Cr-O-Dy ≈ 97.7° at $T_c \approx 23$ K and AFM transition with ∠Cr-O-Dy ≈ 152.1° at $T_N \approx 21$ K occurred. Due to the frustrated spin ground state, a small field (about 0.15 T) induced a metamagnetic transition. On the other hand, in the scheelite phase, an *A*-type-like AFM ordered state was assigned below 24 K, indicating that FM interaction with ∠Cr-O-Dy ≈ 121.1° appeared in the *ab* plane, and AFM coupling with ∠Cr-O-Dy ≈ 132.6° appeared along the *z* axis. As in the zircon phase, a field-induced metamagnetic transition was also observed, but the transition field increased to about 3.0 T.

ACKNOWLEDGMENTS

This work was partly supported by the National Natural Science Foundation and the Ministry of Science and Technology of China through research projects.

*ywlong@aphy.iphy.ac.cn; Present address: Multiferroics Project, ERATO, JST, c/o Cross-Correlation Materials Research Group (CMRG), ASI, RIKEN, Wako, Saitama 351-0198, Japan.

†jin@aphy.iphy.ac.cn

[1] P. A. Lee, N. Nagaosa, and X. G. Wen, Rev. Mod. Phys. **78**, 17 (2006).

[2] M. B. Salamon and M. Jaime, Rev. Mod. Phys. **73**, 583 (2001).

[3] T. Kimura, T. Goto, H. Shintani, K. Ishizaka, T. Arima, and Y. Tokura, Nature (London) **426**, 55 (2003).

[4] Y. W. Long, N. Hayashi, T. Saito, M. Azuma, S. Muranaka, and Y. Shimakawa, Nature (London) **458**, 60 (2009); Y. W. Long, T. Saito, T. Tohyama, K. Oka, M. Azuma, and Y. Shimakawa, Inorg. Chem. **48**, 8489 (2009); Y. W. Long and Y. Shimakawa, New J. Phys. **12**, 063029 (2010).

[5] P. W. Anderson, Phys. Rev. **79**, 705 (1950).

[6] J. B. Goodenough, Phys. Rev. **100**, 564 (1955).

[7] J. Kanemori, J. Phys. Chem. Solids **10**, 87 (1959).

[8] K. Tezuka and Y. Hinatsu, J. Solid State Chem. **160**, 362 (2001).

[9] G. Buisson, F. Tchéou, F. Sayetat, and K. Scheunemann, Solid State Commun. **18**, 871 (1976).

[10] Y. W. Long, Q. Huang, L. X. Yang, Y. Yu, Y. X. Lv, J. W. Lynn, Y. Chen, and C. Q. Jin, J. Mag. Mag. Mater. **322**, 1912 (2010).

[11] M. Steiner, H. Dachs, and H. Ott, Solid State Commun. **29**, 231 (1979).

[12] Y. W. Long, L. X. Yang, Y. Yu, F. Y. Li, R. C. Yu, S. Ding, Y. L. Liu, and C. Q. Jin, Appl. Phys. Lett. **87**, 181901 (2005); J. Phys.: Condens. Matter **18**, 2421 (2006); Phys. Rev. B **74**, 054110 (2006). J. Appl. Phys. **103**, 093542 (2008).

[13] M. B. Smirnov, A. P. Mirgorodsky, V. Yu. Kazimirov, and R. Guinebretière, Phys. Rev. B **78**, 094109 (2008).

[14] Y. W. Long *et al.*, Phys. Rev. B **75**, 104402 (2007).

[15] E. Climent *et al.*, J. Alloys Compd. **488**, 524 (2009).

[16] Y. W. Long *et al.*, J. Am. Chem. Soc. **131**, 16244 (2009).

[17] A. C. Larson and R. B. von Dreele, Los Alamos National Laboratory Report No. LAUR 86-748, 1994 (unpublished).

[18] E. Climent Pascual *et al.*, Phys. Rev. B **81**, 174419 (2010).

[19] J. C. Wright and H. W. Moos, J. Appl. Phys. **41**, 1244 (1970).

[20] A. Kasten, Z. Phys. B **38**, 65 (1980).

[21] E. Jiménez, J. Isasi, and R. Sáez-Puche, J. Solid State Chem. **164**, 313 (2002).

[22] K. Tezuka, Y. Doi, and Y. Hinatsu, J. Mater. Chem. **12**, 1189 (2002).

[23] E. O. Wollan and W. C. Koehler, Phys. Rev. **100**, 545 (1955).